Ultra-Small-Angle X-ray Scattering of a Zinc Sulfonated Polystyrene

Benjamin Chu,*,†,‡ Jian Wang,† Yingjie Li,† and Dennis G. Peiffer§

Chemistry Department, State University of New York at Stony Brook, Stony Brook, Long Island, New York 11794-3400, Department of Materials Science and Engineering, State University of New York at Stony Brook, Long Island, New York 11794-2275, and Corporate Research Science Laboratory, Exxon Research and Engineering Company, Clinton Township, Route 22 East, Annandale, New Jersey 08801

Received January 30, 1992
Revised Manuscript Received May 11, 1992

Morphological structures of ionomers which demonstrate some unique physical properties have been studied extensively.[1-8] Small-angle X-ray scattering (SAXS) of ionomers has revealed the existence of ionic microdomains as evidenced by a broad SAXS peak. Several models[9-11] concerning ionomer morphologies have been proposed to account mainly for the SAXS peak. However, the spatial arrangement of the ionic microdomains which could be estimated from the small-angle upturn has remained one of the open questions. Dynamic viscoelastic measurements of ionomers have demonstrated multiple glass transition temperatures, T_g, one of which has been identified as due to the presence of ionic domains.[7] The distinct appearance of the second T_g for ionic domains supports the supposition that the ionic domains have minimum dimensions of 5–10 nm[12] depending on the techniques used to detect the T_g.

Eisenberg et al.[12] have recently proposed a new morphological model to reconcile the interpretations of mechanical properties and multiphase transitions of ionomers. The Eisenberg model assumes that the multiplets of ions which are the basic units of aggregates are surrounded by a region of polymer backbones with a restricted mobility. When the ion concentration is above a certain value, some overlap of the restricted regions could take place, resulting in ion-rich phases with the multiplets remaining separate from each other. Such a restricted region could act as a hard segment domain and, when large enough, show its own glass transition. This model seems to be more reasonable because it could explain both the multiple glass transition temperatures in a dynamic mechanical spectrum and the ionic peak in a SAXS profile.

It could be difficult to measure the large ionic domain size by using a Kratky collimation system, as the smallest accessible scattering angle is on the order of 1 mrad. The small-angle upturn of an ionomer is usually depicted by a sharp curve, rendering the determination of the initial slope ambiguous. Some efforts have been made[13-15] toward a quantitative description of the small-angle upturn by the Debye–Bueche[16,17] model. Unfortunately, all the Debye–Bueche plots demonstrated no straight lines even at q down to a lowest accessible value of 0.03 nm^{-1}.[14] A question remains whether an initial slope could be determined from the Debye–Bueche plot at sufficiently low q values. In order to further investigate the above question and estimate the size of the overlapped restricted region in the Eisenberg model, we have set up a Bonse–Hart[18,19] camera with an accessible scattering angle down to ~0.25 mrad, equivalent to q = 0.01 nm^{-1}. In this paper we report Bonse–Hart SAXS measurements of 7.4 mol % zinc sulfonated polystyrene (ZnSPS) at room temperature. The Debye–Bueche plot of the ultra-small-angle X-ray scattering (USAXS) data for this sample was analyzed in comparison with the one from an independent measurement using a Kratky camera which had an infinite-slit-length character.

Experimental Section. The polystyrene standard (M_w = 1.05 × 10^5, M_w/M_n = 1.01) was purchased from Polysciences. The sulfonation of polystyrene and the following neutralization by zinc acetate were conducted according to the procedures described in ref 20. The sulfonation content was 7.4 mol % determined by using a Dietert sulfur analyzer. A compression-molded sample film of 0.5 mm in thickness was placed in a vacuum oven at 85 °C for 48 h in order to remove the trace amount of water. The film was then fitted into the sample cell with Kapton (Du Pont Co.) films covering both sides of the sample.

SAXS experiments were performed at the X3A2 State University of New York (SUNY) Beam Line, National Synchrotron Light Source (NSLS), Brookhaven National Laboratory (BNL), using a Bonse–Hart camera which was equipped with two channel-cut germanium crystals aligned in a parallel position. The incident beam was reflected six times from the inner walls of the groove of the first crystal, resulting in a strictly monochromatic beam with a divergence of only several arc seconds. After passing through the sample film, the beam entered into the groove of the second crystal and was reflected six times again before reaching the detector. The second analyzing crystal could be rocked about a horizontal axis around the sample by means of a stepping motor–micrometer assembly that had an angular resolution of 0.1 arc second per step. When the second crystal was rotated by an angle with respect to the sample, only the scattered beam at this angle could enter into the groove of the second crystal and be "seen" by the scintillation detector with a faceplate aperture of 12.7 × 19.1 mm^2.

Results and Discussion. The parasitic scattering and the spreading of the transmitted incident beam very close to the zero scattering angle were extraordinarily minimized by the 12 crystal reflections. The Bonse–Hart camera is often considered as having an infinite slit length due to the groove geometry in the crystals for the strong scattering at very low scattering angles.[21,22] For an infinite slit desmearing, the background-corrected scattered intensity observed experimentally, $I(q)$, is related to the desmeared intensity, $I'(q)$, for the perfect point-focus collimation by the relation[23]

$$I(q) = C\int_0^\infty I'(\sqrt{q^2 + y^2})\,dy \qquad (1)$$

where C is a constant, y is the variable in the detector plane, and q (=$(4\pi/\lambda)\sin(\theta/2)$) is the scattering vector, with θ and λ (=0.154 nm) being the scattering angle and the wavelength, respectively. From the sample-to-air ratio of the main beam intensity at zero scattering angle, the sample absorption could be evaluated. Figure 1 shows the observed scattered intensity curves as a function of scattering vector q ranging from −0.002 to +0.15 nm^{-1} for ZnSPS (circles), air (triangles), and acid sulfonated polystyrene (HSPS; cross signs). The main beam part in the three curves can be clearly identified from the sharp peak in the vicinity of the zero q value. The excess scattered intensity from the ZnSPS sample appeared to be very strong, while the excess scattered intensity from the HSPS sample seemed to be very weak and demonstrated no

* To whom correspondence should be addressed.
† Chemistry Department, State University of New York at Stony Brook.
‡ Department of Materials Science and Engineering, State University at Stony Brook.
§ Exxon Research and Engineering Co.

0024-9297/92/2225-4229$03.00/0

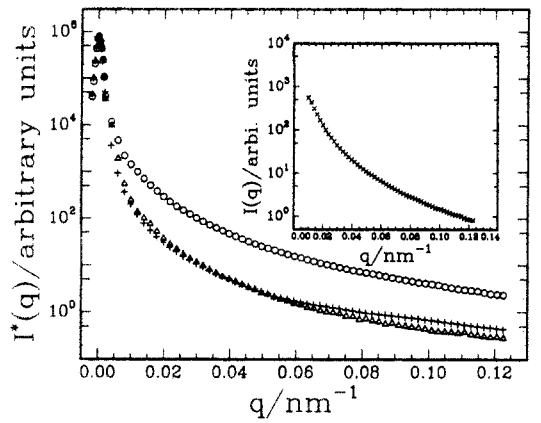

Figure 1. Normalized Bonse–Hart SAXS profiles for ZnSPS (circles), HSPS (cross signs), and air (triangles) at room temperature. The sample absorption was corrected by matching the main beam peak of the sample curves with the peak of the air curve at zero q by means of vertical rescaling. The inset is the difference pattern obtained by subtracting the HSPS curve from the ZnSPS curve. $I^*(q)$ denotes the scattered intensity without background correction.

discernible difference in comparison with the air scattering. The inset shows the difference scattering profile which was obtained by subtracting the HSPS curve from the ZnSPS curve. It should be noted that at such small scattering angles the residual scattering from the optical elements and the voids or the impurities due to poor sample film preparations might contribute to the USAXS profile. We used a difference scattering profile between the ZnSPS and the HSPS so that the contributions to the scattered intensity arising from the voids or the impurities could possibly be canceled out. The same scattering profile as the one in the inset of Figure 1 was obtained when we used the air scattering curve instead of the HSPS scattering curve as the background.

For an inhomogeneous system, the Debye–Bueche model can be employed to describe the inhomogeneity in terms of a correlation length. An exponential form for the correlation function, which relates the local electron density fluctuations at points a and b, is given by

$$\gamma(r) = \exp(-r/\xi) \tag{2}$$

where r is the distance between points a and b and ξ is the correlation length which is a measure of the ionic domain size. A Fourier transform of $\gamma(r)$ leads to an equation for the scattered intensity from the perfect point-focus beam:

$$I'(q) = \frac{A'}{(1 + \xi^2 q^2)^2} \tag{3}$$

where A' is a constant. For the infinite slit-smeared scattered intensity, the Debye–Bueche model can be corrected, according to eq 1, by integrating eq 3 over the variable y of the slit length:

$$I(q) = A' \int_0^\infty \frac{dy}{[1 + \xi^2(q^2 + y^2)]^2} = \frac{A}{(1 + \xi^2 q^2)^{3/2}} \tag{4}$$

where A is a new constant. The correlation length can be determined from the Debye–Bueche plot of $I^{-2/3}$ versus q^2 for the infinite-slit smearing data. Figure 2a shows the Debye–Bueche plot for 7.4% ZnSPS (open circles) deduced from the data in the inset of Figure 1. A somewhat straight line was observed. However, this linear curve may not really suggest that the Debye–Bueche model is satisfactory for the description of the present USAXS curve because (1) the curvature was still visible at q even down to 0.01 nm^{-1} as amplified by an alternative plot shown in Figure 2b and (2) the assumption of an infinite slit length for the

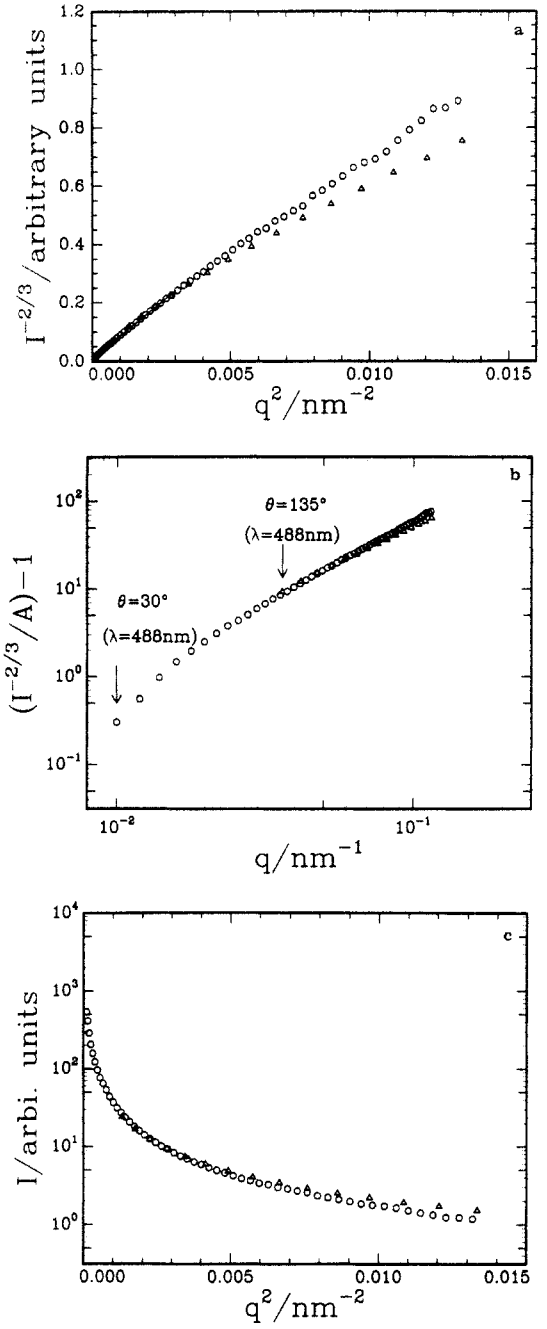

Figure 2. (a) Debye–Bueche plot of $I^{-2/3}$ vs q^2. Circles denote the data obtained from the Bonse–Hart camera, and triangles denote the data obtained from the Kratky camera using an infinite-slit-length geometry. (The symbol meanings also apply to parts b and c.) The solid line represents the least-squares fitting of the initial slope, from which the correlation length was estimated to be ~90 nm. (b) log–log plot of $(I^{-2/3}/A) - 1$ vs q to demonstrate the quality of our USAXS data. A curvature is noted even at q down to 0.01 nm^{-1}. (c) Guinier plot of log I vs q^2 for ZnSPS at room temperature.

Bonse–Hart camera used in the synchrotron X-ray source broke down as a result of the focusing characteristics of the synchrotron main beam. In order to check the infinite-slit-length assumption, an independent measurement of the same 7.4% ZnSPS was carried out by using a Kratky camera with a regular X-ray generator. The Kratky camera was set to obey the infinite-slit-length geometry.[24] The Kratky camera data are also shown in Figure 2 as hollow triangles. An obvious difference in the shape of the SAXS profiles is noticed, implying that the general infinite-slit-length assumption for the Bonse–Hart camera with a synchrotron X-ray source is not satisfactory over the angular range covered by a conventional Kratky

camera. Nevertheless, the two curves tend to merge together as the scattering angle becomes smaller because the infinite-slit-length assumption becomes more acceptable at lower q values. Thus, an estimation of the correlation length from the initial slope of the Bonse–Hart data in Figure 2a yields a value of ~90 nm, which is comparable with that reported by other authors[13] but is larger than that reported previously by some of the present authors using a modified Kratky camera.[14] Undoubtedly, the correlation length value for an ionomer would vary largely depending on the q range as a consequence of the persistent concave downward shape of the SAXS profile in a Debye–Bueche plot. In any case, the large correlation length value might serve as an estimate of the size of the overlapped restricted region of ion-rich phases as postulated by Eisenberg et al.[12] It is interesting to note from Figure 2b that the q range based on light scattering with λ = 488 nm and θ between 30° and 135° is within the capability of our Bonse–Hart camera using an X-ray wavelength of 0.154 nm. The difference between the two curves is less obvious in a log–log plot.

The Guinier approximation could also be tested. The expression for the smeared scattered intensity has the same form as that for the desmeared scattered intensity:[23]

$$I(q) = \alpha \exp(-\beta q^2) \quad (5)$$

where α and β ($=R^2/3$) are constants, with R being the radius of gyration of the particles. Figure 2c shows Guinier plots for the same data as in Figure 2a. Apparently, the inhomogeneous structures of the ionomer under study do not follow the Guinier model. One of the reasons could be due to the polydisperse distribution of the inhomogeneous structure dimensions.

Conclusion. A Bonse–Hart camera in combination with a synchrotron X-ray source has been used to determine the long-range inhomogeneity of 7.4 mol % ZnSPS. The infinite-slit-length assumption for the Bonse–Hart camera used in a synchrotron X-ray source was found to break down at large q values accessible by the Kratky camera. The Debye–Bueche plot for this ionomer showed a downward bending even at q down to 0.01 nm^{-1}. The correlation length was estimated to be on the order of ~90 nm. This large correlation length could be considered to be a supportive evidence for the Eisenberg model. A detailed study on the ionomer long-range inhomogeneities using a Bonse–Hart camera with a well-defined slit-length geometry is under way.

Acknowledgment. B.C. greatly acknowledges the Polymers Program, National Science Foundation (Grant DMR8921968), the U.S. Army Research Office (Grant DAALO391G0040), and the U.S. Department of Energy (GrantsDEFG0286ER45237A005andDEFG0589ER75515) for support of this research.

References and Notes

(1) Holliday, L., Ed. *Ionic Polymers*; Applied Science Publishers: London, 1975.
(2) Eisenberg, A.; King, M. *Ion-Containing Polymers*; Academic Press: New York, 1977.
(3) Wilson, A. D., Prosser, H. J., Eds. *Developments in Ionic Polymers-1*; Applied Science Publishers: Barking, U.K., 1983.
(4) MacKnight, W. J.; Lundberg, R. D. *Rubber Chem. Technol.* **1984**, *57*, 652.
(5) Pineri, M., Eisenberg, A., Eds. *Structure and Properties of Ionomers*; NATO ASI Series 198; D. Reidel Publishing Co.: Dordrecht, Holland, 1987.
(6) Tant, M. R.; Wilkes, G. L. *J. Macromol. Sci. Rev.* **1988**, *C28*, 1.
(7) Fitzgerald, J. J.; Weiss, R. A. *J. Macromol. Sci. Rev.* **1988**, *C28*, 99.
(8) Lantman, C. W.; MacKnight, W. J.; Lundberg, R. D. *Annu. Rev. Mater. Sci.* **1989**, *19*, 295.
(9) MacKnight, W. J.; Taggart, W. P.; Stein, R. S. *J. Polym. Sci., Polym. Symp.* **1974**, *45*, 113.
(10) Fujimura, M.; Hashimoto, T.; Kawai, H. *Macromolecules* **1981**, *14*, 1309.
(11) Yarusso, D. J.; Cooper, S. L. *Macromolecules* **1983**, *16*, 1871.
(12) Eisenberg, A.; Hird, B.; Moore, R. B. *Macromolecules* **1990**, *23*, 4098.
(13) Ding, Y. S.; Hubbard, S. R.; Hodgson, K. O.; Register, R. A.; Cooper, S. L. *Macromolecules* **1988**, *21*, 1698.
(14) Wu, D.; Phillips, J. C.; Lundberg, R. D.; MacKnight, W. J.; Chu, B. *Macromolecules* **1989**, *22*, 992.
(15) Register, R. A.; Cooper, S. L. *Macromolecules* **1990**, *23*, 310.
(16) Debye, P.; Bueche, A. M. *J. Appl. Phys.* **1949**, *20*, 518.
(17) Debye, P.; Anderson, H. R., Jr.; Brumberger, H. *J. Appl. Phys.* **1957**, *28*, 679.
(18) Glatter, O., Kratky, O., Eds. *Small Angle X-ray Scattering*; Academic Press: London, 1982; and references cited therein.
(19) Chu, B.; Li, Y.; Gao, T. *Rev. Sci. Instrum.*, to be published.
(20) Lundberg, R. D.; Makowski, H. S. *J. Polym. Sci., Polym. Phys. Ed.* **1980**, *18*, 1821.
(21) Gravatt, C. C.; Brady, G. W. *J. Appl. Crystallogr.* **1969**, *2*, 289.
(22) Dwiggins, C. W., Jr. *J. Appl. Crystallogr.* **1979**, *12*, 401.
(23) Guinier, A.; Fournet, G. *Small-Angle Scattering of X-rays*; John Wiley & Sons: New York, 1955.
(24) Kratky, O. In *Small-Angle X-ray Scattering*; Brumberger, H., Ed.; Gordon & Breach: New York, 1966; p 94.